

Larson Miller Parameter for the Prediction of the Creep Life of Unweld and Welded P91 Steel

S.N.A. Rosli¹, N. Ab. Razak^{1*}, N.A Alang¹

¹Structural Performance and Materials Engineering (SUPREME) Focus Group, Faculty of Mechanical and Automotive Engineering Technology, Universiti Malaysia Pahang, 26600, Pekan, Pahang, MALAYSIA.

DOI: <https://doi.org/10.30880/ijie.2022.14.08.013>

Received 30 May 2022; Accepted 28 November 2022; Available online 21 December 2022

Abstract: For structural components that operate at elevated temperatures, martensitic P91 steel is preferable. It is widely used in steam generators in the fossil-fired thermal and nuclear power generation sectors due to its creep endurance and corrosion resistance. Several creep laws, such as Monkman-Grant, Theta project, Wilshire and Sinh model, Omega technique, and the Larson Miller Parameter (LMP), have been developed over time to predict and failure of materials susceptible to the creep phenomenon. However, only the Omega Law and Larson-Miller Parameter are the only two methods approved in API 579-1. In this work, the creep test for welded and unwelded P91 were conducted at temperatures of 600°C under stresses of 165, 175 MPa, and 190 MPa. In comparison to the welded specimens, the unwelded specimens displayed a continuously more substantial development of creep strain with time, resulting in a higher steady-state creep rate and a shorter rupture life. The increased magnitude of creep-rupture data has been observed to impact the dependability of creep life. Because of more significant changes in service temperature and stress conditions, the dependability of P91 steel has deteriorated, as well as an increase in creep life. The rupture life has been predicted using the LMP method, which utilizes the constant C parameter. At the same stress, the predicted creep life for weld material shows a higher value than that of the parent material, which is consistent with the experimental result.

Keywords: Creep behaviour, P91 steel, and Larson Miller parameter

1. Introduction

P91 steel is renowned for its use in high-temperature environments such as steam generators in the fossil-fired thermal and nuclear power generation sectors [1–3]. P91 steel is made by adding nitrogen (N) to a formula that already contains strong carbide/nitride producing components like vanadium and niobium [4] thus exhibiting superior mechanical qualities at increased temperatures compared to 9Cr–1Mo steel [5–8]. The most advanced steam power plants attain an efficiency of around 42 percent at steam temperatures of 650°C [9]. Thus, high thermal efficiency without sacrificing boiler and turbine component reliability and service life necessitates using more robust materials capable of functioning under severe stresses at rising temperatures.

Although P91 steel is a favourable material for high-temperature usage, prolonged exposure to service, or severe overheating, the majority of the fractures occurred in the weldment rather than the base metal. Weldments, which are made up of the parent material (PM), the weld metal (WM), and the heat affected zone (HAZ), which are all discrete zones with differing microstructures, have been reported to have had these failures. The creep nucleation, propagation and damage accumulation rate is frequently at its highest in the vicinity of the HAZ [10]. The HAZ region is separated into three distinct subregions: the coarse-grained zone, the fine-grained zone, and the intercritical zone. After long-term operation, creep fracture in the fine-grained HAZ regions of Grade 91 weldments has recently become a global issue for Grade P91 steel. Therefore, the requirement for life evaluation of components in the creep range is of major relevance.

Numerous life prediction techniques, such as the Theta project [11], the Kachanov approach [12], the Larson Miller Parameter [13], and the Omega method [14], have been developed to guarantee its safety at high temperatures. API 579-1/ASME FFS-1, on the other hand, only acknowledges the Omega methodology and the Larson Miller (LMP) method. Prager [15] has developed the idea for the MPC project, which is now known as The Omega model. The Omega method has been approved for incorporation into API RP579 on fitness-for-service [16]. The Omega model permits the estimation of the remaining service life of a component in the creep regime at elevated temperatures and pressures. The Omega parameters, consisting of a strain rate and a multi-axial damage parameter, are utilized to predict the rate of strain accumulation, creep damage accumulation, and remaining time to failure as a function of stress state and temperature.

The most prevalent extrapolation approach for determining the creep life of metals is the Larson Miller Parameter. The Larson-Miller parameter (P) is expressed experimentally in this manner as $P = T [C + \log(t)]$, where C is a constant. An extension of the plot of $\log(t)$ vs. $1/T$ reveals that the isostress lines intersect the vertical axis at $1/T = 0$, which is proportional to the Larson-Miller constant C, providing support for this hypothesis. According to the data, it is uncommon for iso-stress lines to intersect at a single location.

The steel undergoing a thermally induced creep process of stress rupture can have its equivalence of time at temperature represented by the Larson-Miller parameter. LMP can predict equivalent times required for stress rupture at different temperatures. This method of extrapolating stress rupture and creep data assumes that each material should have a unique value for the absolute temperature-compensated time function. This value can be altered only by the amount of force applied.

The goal of this work is to examine the weld and unwelded P91 material creep behaviour, as well as to anticipate the creep life of P91 using LMP techniques. Creep experiments were performed at 600°C on welded and unwelded P91 steel at two distinct stresses: 175 MPa and 190 MPa.

2. Material

This work made use of P91 steel material. The material’s chemical constituents are listed in Table 1. Oxford Foundry-Master UV was used to analyse the chemical compositions. Prior to testing, the P91 steel was metallographically examined. The metallographic sample was then polished following sectioning, mounting, grinding, and polishing. The sample was then etched using Vilella Reagent. Fig. 1 reveals the results of an optical microscope analysis of an etched sample. Microstructure analysis of P91 steel revealed that it was composed of tempered martensite with infrequent stringer-like nonmetallic inclusions, as seen in Fig. 1.

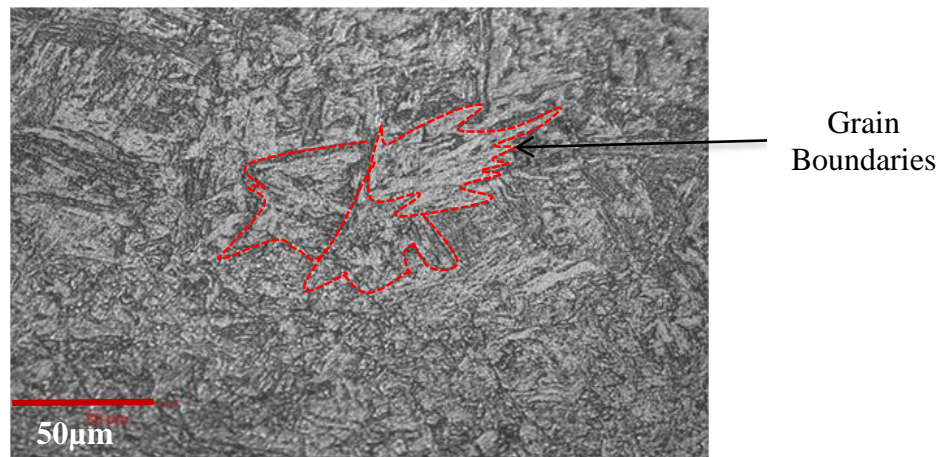


Fig. 1 - Microstructure of parent P91

Table 1 - Chemical composition of P91 steel

Element	Cr	Mo	Mn	Si	V	C	Cu	N	N/Al	Nb	Co
Amount (wt%)	8.79	0.99	0.38	0.41	0.23	0.11	0.10	0.05	0.05	0.04	0.02

3. Experimental Setup

For welded P91, the welding procedures were conducted using the SMAW method according to ASME IX [17]. The pipe had a Single Vee Butt Weld, and the electrode/consumables used for the experiment were ER90S-B9.. After the P91 components are welded, post-weld heat treatment (PWHT) is compulsory to alleviate internal stresses and temper fresh martensite while forming desirable MX-precipitate phases distributions in conjunction with AS4458 & ASME 31.1.

During the application of the required PWHT, the precipitate phases and substantiate distribution at close vicinity to the fusing line are formed. The preheating temperature was 200°C, and the maximum interpass temperature was 300°C prior to weld. Fig. 2 shows the dimension of the welded pipe. The specimens for both unwelded and weld material for the creep testing were machined at 36mm gauge length, as illustrated in Fig. 3. The specimens were machined with the longitudinal axial parallel to the pipe axis, and the gauge length centred on the weld. The actual creep specimens of welded and unwelded P91 with a 36 mm gauge length are depicted in Fig. 4.

The creep machine used was equipped with primary components including the furnace and device for recording data. The test specimen was placed within the creep machine. The specimen was heated up to desired temperature and recorded by a top, middle, and bottom thermocouples that were installed on the furnace wall. The experiment was monitored to keep temperatures within 2 degrees Celsius. Fig. 5 shows a thermocouple-equipped specimen close-up. A linear variable differential transformer (LVDT) was used to measure the material's elongation along its longitudinal axis. The LVDT was placed in the middle of two aluminium plates. The elongation were recorded throughout the test, as soon as the specimen fractured, the test was terminated. The creep rupture test was carried out using the recommended procedure developed by ASTM E139-11 [18]. Both welded and unwelded P91 were subjected to creep temperature at 600°C and stresses, 175 MPa, and 190 MPa.

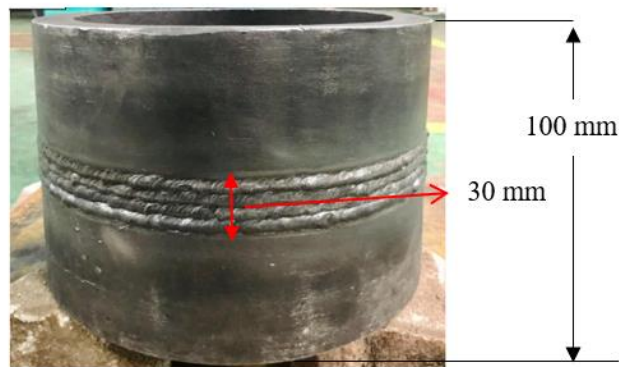


Fig. 2 - Dimension of welded pipe

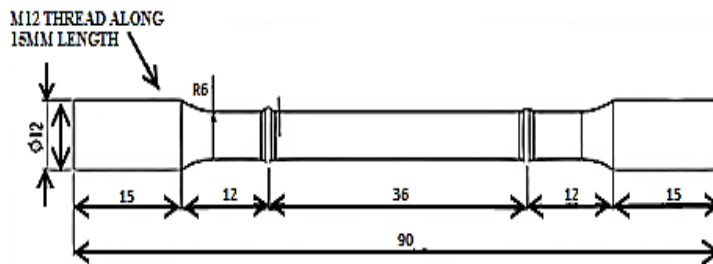


Fig. 3 - Dimension of uniaxial creep test specimen



Fig. 4 - P91 Uniaxial creep specimen

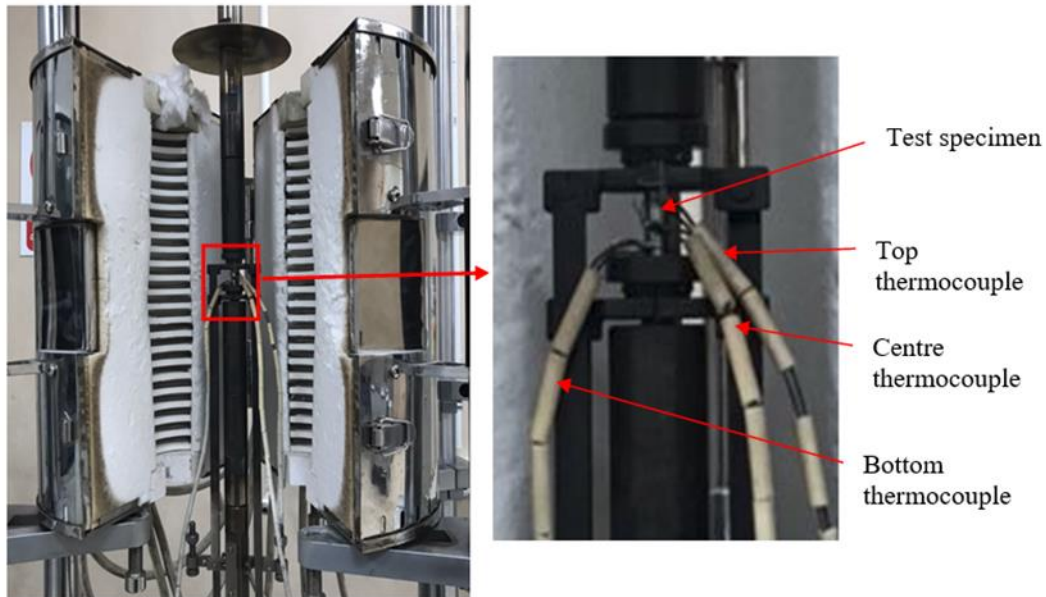


Fig. 5 - Test specimen setup in the furnace and closed- up view of thermocouple setup

3.1 Larson-Miller Parameter

The P91 metal material’s stress value is often low in actual operating conditions. In order to shorten test time, accelerated test procedures, such as raising the temperature and applying stress, are commonly used in the laboratory. The extrapolation approach is then used to anticipate the actual service life of the material. Thus, the dependability of the results dramatically depends on the testing technology and extrapolation technique. The Larson-Miller parameter is a well-known extrapolation method. The fundamental principle of this approach is that when the temperature increases, the creep life decreases while the stress value remains constant. Despite this, the value of the Larson-Miller parameter does not change. If the steady creep stage corresponds to the Arrhenius law, then, the minimum creep rate (steady creep rate) is denoted by $\dot{\epsilon}_{min}$, A is the constant, Q_c is the creep activation energy, R is the gas constant, and T is the absolute temperature. The relationship between the rupture time and minimum creep rate is as follows:

$$\dot{\epsilon}_{min} = A \exp\left(-\frac{Q_c}{RT}\right) \quad t_r \dot{\epsilon}_{min} = C \quad (1)$$

$$t_r \dot{\epsilon}_{min} = C \quad (2)$$

Where t_r represents the creep rupture life and C is the Larson-Miller constant. According to Srinivasan et al., the phenomenally determined and usually suggested value of C is 33. Rearranging the eq. (1) and (2), then:

$$\left(\frac{Q_c}{RT}\right) = T (C + \log t_r) \quad (3)$$

Eq. (3) is usually written as,

$$P_{LM} = T (C + \log t_r) \quad (4)$$

P_{LM} stands for the Larson-Miller parameter. Eq. (4) under fixed stress conditions may be expressed as:

$$\log t_r = P_{LM} \left(\frac{1}{T}\right) - C \quad (5)$$

4. Experimental Result

Along the 60 mm position of hardness test are consists of the P91 parent metal, fusion zone and heat affected zone (consist of three types ; Coarsed-Grained HAZ (CGHAZ), Fine-Grained HAZ (FGHAZ), and Intercritical HAZ (ICHAZ)

as shown in Fig. 6. At each position, the hardness are measured 5 times, thus able to obtained the average hardness value as tabulated in Table 2. As expected for P91 steel, the base metal has the lowest hardness value of 219.3HV and 234.5HV at 60 mm and 0 mm position, respectively. The hardness of the HAZ showed a notable rise to 314.3 HV. These hardness values are consistent with the findings of D.M. Madyira et al. [19] which suggested the high hardness value in HAZ is due to the heat input used for welding caused residual strains in the weldments [19]. The HAZ is a common location for type III and IV cracking, which can impair the mechanical performance of P91 weldments when used in a power plant.

Table 2 - P91 average hardness values at different location

Position(mm)	Average Hardness (HV)
0	234.5
15	262.8
30	314.3
45	243.0
60	219.3

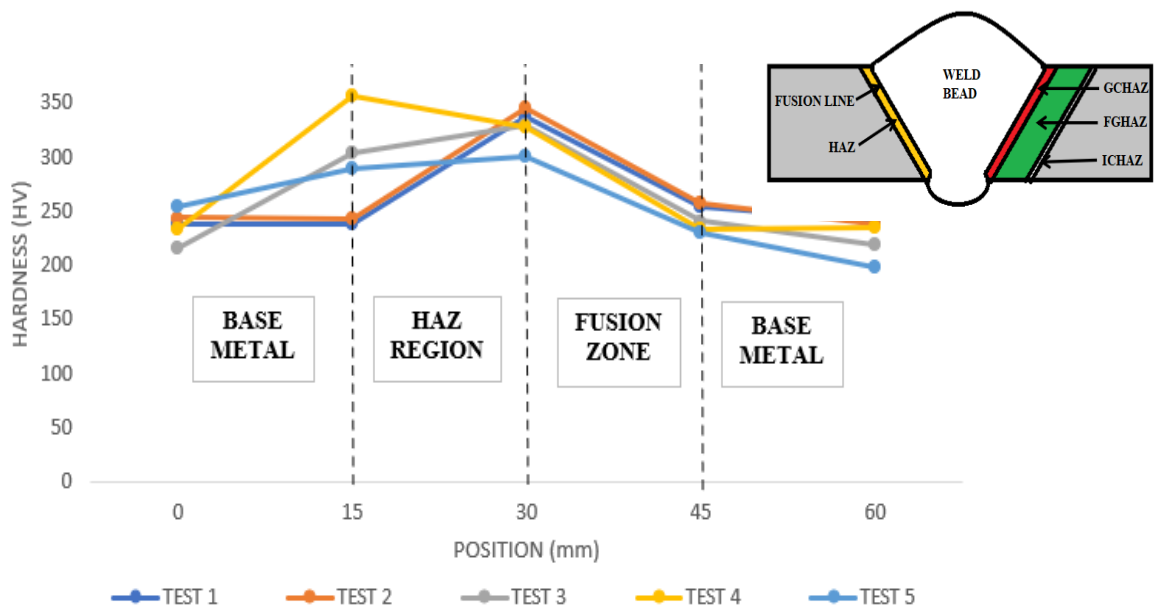


Fig. 6 - Combined P91 hardness profiles

4.1 Result of Creep

Figs. 7 and 8 show the graph of creep strain against time for welded and unwelded P91 steel specimens at a temperature of 600°C and stress of 175 MPa and 190 MPa, respectively. Both creep curves of Fig. 7 and Fig. 8 exhibit the typical creep strain versus time curve conditions which consist of primary, secondary, and tertiary stages. As can be seen in Fig. 7, at the temperature of 600°C with lower stress (175 MPa), the unwelded P91 creep specimen has a higher creep strain compared to welded P91 specimen. However, it also showed that unweld specimens have a slightly shorter time to rupture. For example, the unweld creep specimen at 600°C and 175 MPa was 242.54 h, whereas the weld creep specimen ruptured after 255.05 h. The difference in time rupture was only 12.51 hours. Creep deformation of P91 steel at 190 MPa and 600°C is shown in a typical creep curve for weld and unweld specimen circumstances in Fig. 8. In the presence of significant loads, the primary creep is reduced to a negligible value, and creep curves are short. Compared to the results obtained for welded creep specimen condition, the steady state creeps rate and rupture life of the unweld creep specimens were consistently higher. It is fascinating to see that all the tests behave similarly in principle, regardless of how long it takes them to fail. Similar results were found for martensitic materials [20,21].

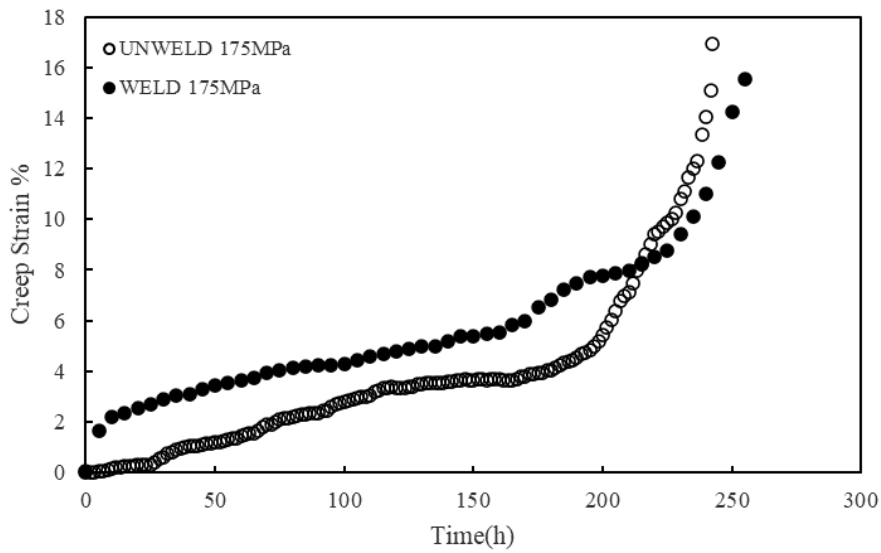


Fig. 7 - Creep strain-time plots of welded and unwelded P91 heat-resistant steel at 175 MPa

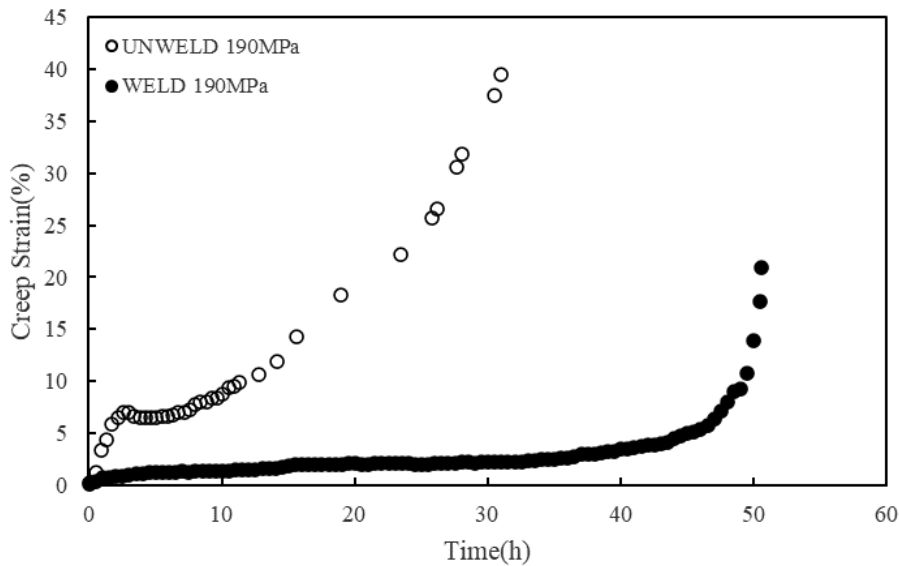


Fig. 8 - Creep strain-time plots of welded and unwelded P91 heat-resistant steel at 190 MPa

Table 3 tabulated the creep rupture time and minimum creep strain rate for the weld and unwelded P91 material. As the stress decreases at 600 °C, the minimum creeps rate decreases while the rupture duration increases. Figs. 10 –12 show the creep strain and strain rate for the weld and unwelded P91 at 175 MPa and 190 MPa. In the creep curve, the secondary creep zone is where the creep rate is lowest. Fig. 16 and Fig. 17 show the necking of welded and unwelded P91 steel uniaxial round bar for stress at 190 MPa. Fig. 16 shows that the creep specimen necking happens at approximately 45 degrees; the degree of the necking shows it is significant to the HAZ region. The welded creep specimen ruptures at 50.60 hours. In Fig. 17, the creep specimen shows a typical necking of an unwelded creep specimen which ruptures at 31.33 hours.

Table 3 - Creep result of P91

Temperature T/°C	Stress σ /Mpa	Material	Rupture time t/h	Minimum creep rate (ϵ' min)
600°C	175	Weld	255.05	8.63×10^{-4}
		Unweld	242.54	1.91×10^{-3}
	190	Weld	50.60	4.60×10^{-3}
		Unweld	31.33	2.50×10^{-2}

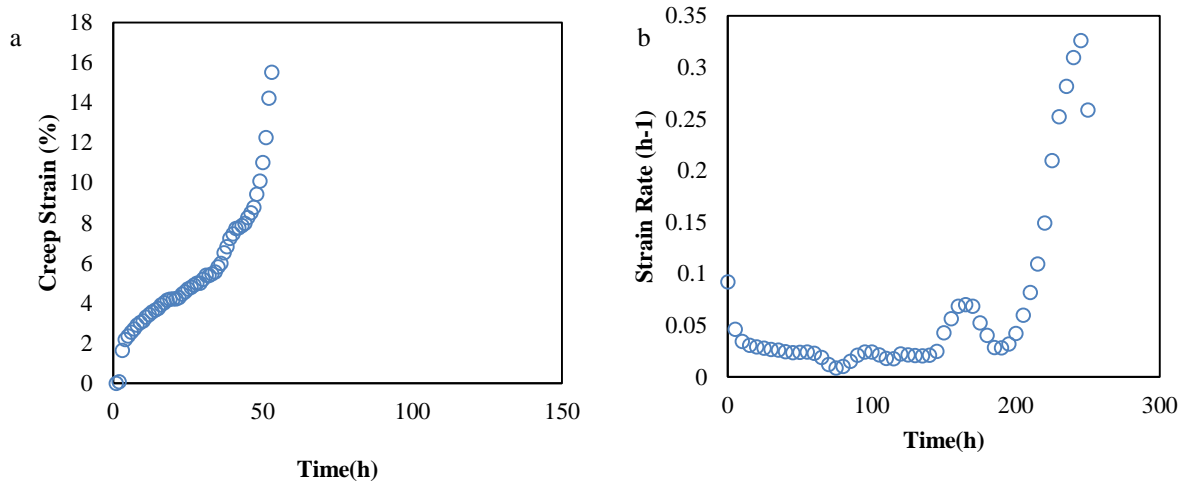


Fig. 9 - (a) Creep strain and; (b) strain rate data of welded P91 at 175 Mpa

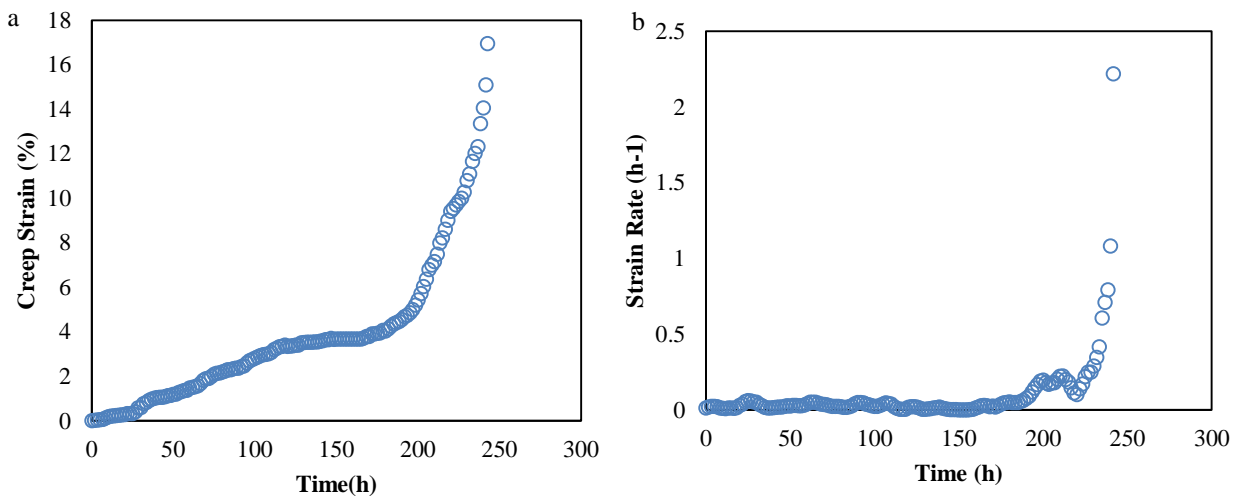


Fig. 10 - (a) Creep strain and; (b) strain rate data of unwelded P91 at 175 MPa

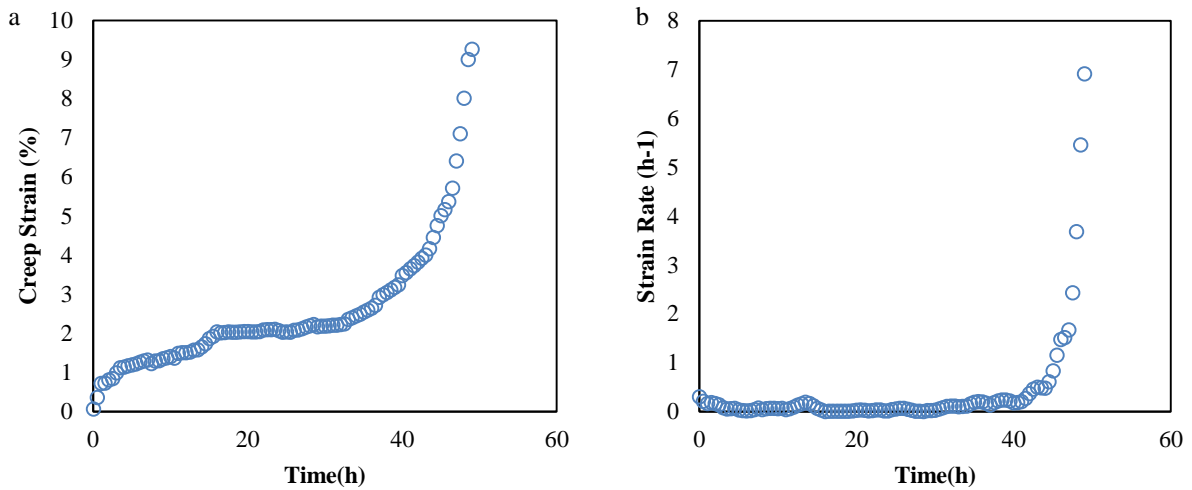


Fig. 2 - (a) Creep strain and; (b) strain rate data of welded P91 at 190 MPa

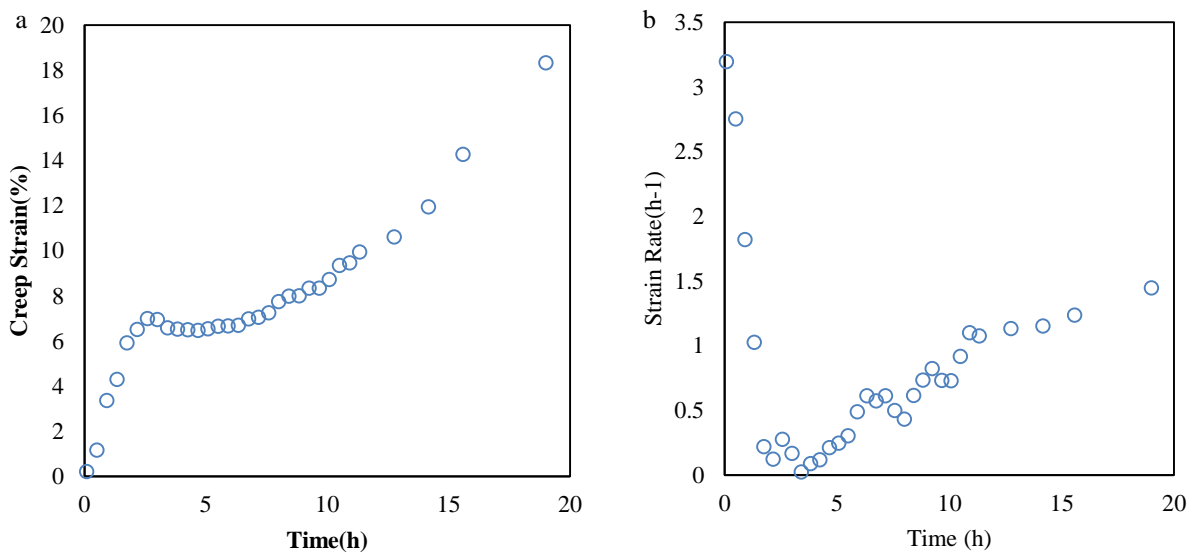


Fig. 32 - (a) Creep strain and; (b) strain rate data of unwelded P91 at 190 MPa



Fig. 4 - Rupture of P91 steel uniaxial round bar for the stress of welded 190 MPa at 50.60 hours



Fig. 5 - Rupture of P91 steel uniaxial round bar for the stress of unwelded 190 MPa at 31.33 hours

4.2 Predicted Result By Using Larson-Miller Parameter

Due to constrains in both time and material resources, the creep tests performed on the unwelded and weld material in this work were limited. In order to more fully characterise the material over a longer time period, the available literature

data [22] were compared and analysed with the current test data. The correlation between stress and rupture time for experimental and published data tested at 600 °C is shown in Fig. 15. The experimental data for accelerated tests carried out at high stresses (165 MPa to 190 MPa) are included in the data set, as shown in the figure. As can be seen, the data exhibit a power relation between 100 and 10,000 hours, but at longer creep lives, the data show a sharp decline in creep strength. The ability to predict a rupture under relatively low stress over an extended period is crucial because it simulates the real operation of a power plant. It is predicted for temperatures changes from 600 to 650°C, there appears to be a change in the creep strength after 10,000 hours. Due to microstructural changes, the subgrain size increased gradually and then suddenly prior to creep failure, the creep rupture strength significantly decreased [23].

In this study, Larson Miller parameter was utilised to predict the creep life. The Larson-Miller equation shows that under various stress circumstances it can be used to forecast the creep rupture life of P91 steel. With this technique, the idea of a time-temperature grouping with the formula $T(C+\log tR)$ was introduced. The ability to draw a family of rupture curves representing various test temperatures for a given material on a new temperature-compensated time axis (Larson-Miller parameter axis) and superimpose them all on a single master curve is well recognised. Fig. 19 shows the plot of LMP versus the stress for both the unweld and weld experimental data. The literature data (unweld)[22] are plotted in the same plot to analyse the LMP parameter and provide confidence in the data set. The dashed line and dotted line represent the best fit obtained for the weld and unweld material. For all cases, the constant $C=30$ was used which was the best fit value for Grade 91 steel [24]. Although the experimental data is limited, the experimental data for unweld are in good agreement with the literature data. Both plots show that the creep life decreases with the increase of stress. For example, at 2000h, the expected creep life for weld material yields more stress than the unwelded material, which is consistent with the experimental result. The Larson-Miller extrapolation may overestimate the long-term creep life due to the material degrading phenomena that cause premature failure [24,25].

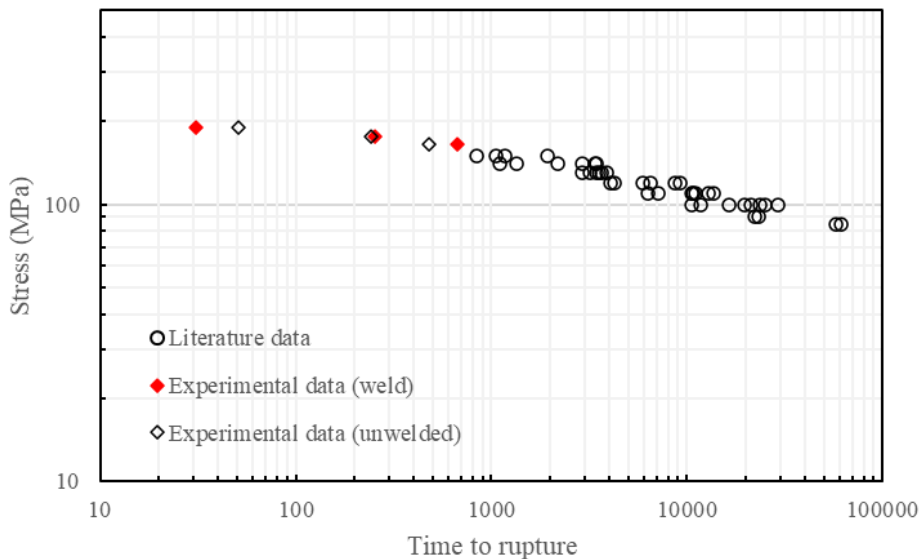


Fig. 6 - Plot of stress versus rupture time for both the unweld and weld experimental data

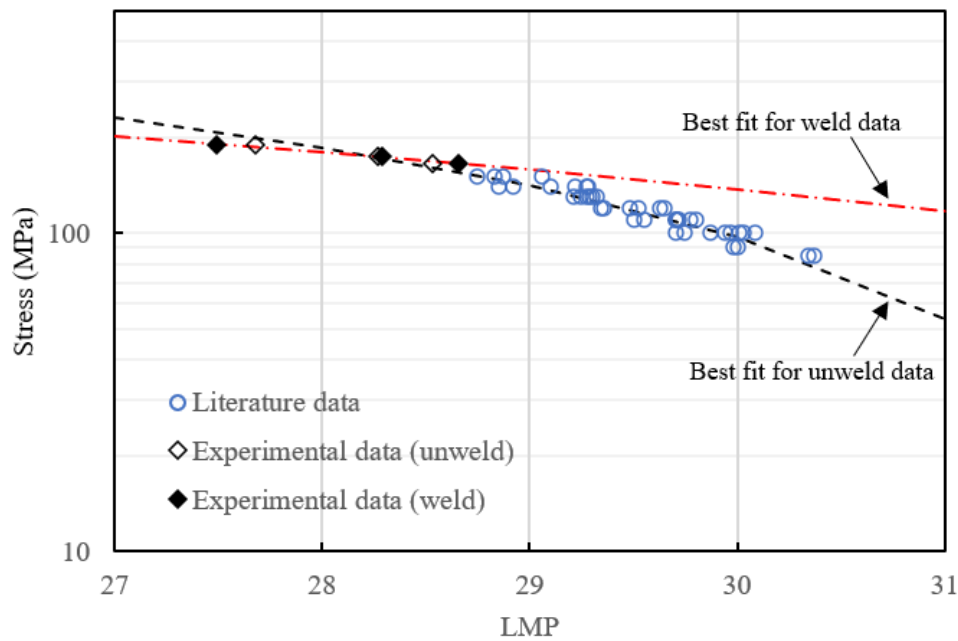


Fig. 16 - Plot of LMP versus the stress for both the parent and weld experimental data

5. Conclusion

In this work, the creep tests were performed at temperatures of 600°C under the stresses of 165 to 190 MPa on P91 steel. This leads us to the following findings.

- Rupture of P91 steel uniaxial round bar for the stress of welded 175 MPa at 255.05 hours meanwhile, rupture of P91 steel uniaxial round bar for the stress of unwelded 175 MPa at 242.54 hours.
- Rupture of P91 steel uniaxial round bar for the stress of welded 190 MPa at 50.60 hours meanwhile rupture of P91 steel uniaxial round bar for the stress of unwelded 190 MPa at 31.33 hours.
- As shown in stress vs rupture time, at longer creep lives, the data show a sharp decline in creep strength which predict a rupture under relatively low stress over an extended period of time
- The experimental data for unwelded material are in good agreement with the literature data. Both plots show that the creep life decreases with the increase of stress. The Larson-Miller extrapolation may overestimate the long-term creep life due to the material degrading phenomena that cause premature failure.

Acknowledgement

To the Malaysian Ministry of Higher Education (MOHE) and Universiti Malaysia Pahang, The authors are grateful to the internal grant FRGS/1/2019/TK03/UMP/03/5 for financing this study. Facility use was provided by the UMP Faculty of Mechanical and Automotive Engineering Technology.

References

- [1] Kim, W. G., Park, J. Y., Yin, S. N., Kim, D. W., Park, J. Y., et al. (2011). Reliability Assessment of Creep Rupture Life for Gr.91 Steel by an Interference Model. Volume 6: Materials and Fabrication, Parts A and B, ASMEDC.
- [2] Spigarelli, S., & Quadri, E. (2002). Analysis of the creep behaviour of modified P91 (9Cr-1Mo-NbV) welds, *Materials & Design*, 23(6), 547–52.
- [3] Wang, H., Gao, P., Turner, R., Chen, H., Qi, L., & Yang, B. (2020). Constitutive modelling for strain hardening alloys during isothermal compression: An efficient semi-empirical method coupling the effects of strain, temperature and strain-rate, *Mater. Today Commun.*, 24, 101040.
- [4] Choudhary, B.K., Kim, W.-G., Mathew, M.D., Jang, J., Jayakumar, T., & Jeong, Y.-H. (2014). On the Reliability Assessment of Creep Life for Grade 91 Steel, *Procedia Eng.*, 86, 335–41.
- [5] Abe, F., Noda, T., Araki, H., & Nakazawa, S. (1991). Alloy composition selection for improving strength and toughness of reduced activation 9Cr-W steels, *Journal of Nuclear Materials.*, 179–181, 663–666.
- [6] Mannan, S.L., Chetal, S.C., Raj, B., & Bhoje, S.B. (2003). Selection of materials for prototype fast breeder reactor, *Trans. Inst. Met.*, 56(2), 155–78.

- [7] Raj, B., & Choudhary, B.K. (2010). A perspective on creep and fatigue issues in sodium cooled fast reactors, *Trans. Indian Inst. Met.*, 63(2–3), 75–84.
- [8] Choudhary, B.K., & Isaac Samuel, E. (2011). Creep behaviour of modified 9Cr–1Mo ferritic steel, *Journal of Nuclear Material.*, 412(1), 82–89.
- [9] Zhang, Y. (2009). Changes in microstructure and mechanical properties of P91 weld metal during creep, .
- [10] Hyde, T.H., & Sun, W. (1998). Creep of welded pipes, *Proceedings of the Institution of Mechanical Engineers: Part E: Journal of Process Mechanical Engineering.*, 212(3), 171–82.
- [11] Zheng, Y., Yang, S., & Ling, X. (2017). Creep life prediction of small punch creep testing specimens for service-exposed Cr5Mo using the theta-projection method, *Engineering Failure Analysis*, 72, 58–66.
- [12] Mandziej, S.T., & Výrostková, A. (2008). Evolution of Cr-Mo-V Weld Metal Microstructure During Creep Testing-Part 1: P91 Material, *Welding in the World*, 52(1–2), 3–26.
- [13] Liang, T., Liu, X., Fan, P., Zhu, L., Bi, Y., & Zhang, Y. (2020). Prediction of long-term creep life of 9Cr–1Mo–V–Nb steel using artificial neural network, *International Journal of Pressure Vessels & Piping*, 179, pp. 104014.
- [14] Prager, M. (2000). The Omega Method-An Engineering Approach to Life Assessment, *Journal of Pressure Vessel Technology*, 122(3), 273–80.
- [15] Prager, M. (1995). Development of the MPC Omega Method for Life Assessment in the Creep Range, *Journal of Pressure Vessel Technology*, 117(2), pp. 95–103.
- [16] Anderson, T.L. & Osage, D.A. (2000). {API} 579: a comprehensive fitness-for-service guide, *International Journal of Pressure Vessels & Piping*, 77(14–15), pp. 953–63
- [17] Boiler, A., Code, P.V. (1968). Section IX, ASME, New York.
- [18] (N.d.). Test Methods for Conducting Creep, Creep-Rupture, and Stress-Rupture Tests of Metallic Materials.
- [19] Madyira, D.M., Liebenberg, J.A., & Kaymacki, A. (2017). Comparative Characterization of P91 and 10CrMo9-10 Creep Resistant Steel Welds, *Procedia Manufacturing*, 8, 345–52.
- [20] Shrestha, T., Basirat, M., Charit, I., Potirniche, G.P., & Rink, K.K. (2013). Creep rupture behavior of Grade 91 steel, *Material Science & Engineering: A*, 565, 382–391.
- [21] Choudhary, B.K. (2013). Tertiary creep behaviour of 9Cr–1Mo ferritic steel, *Material Science & Engineering: A*, 585, pp. 1–9.
- [22] Sawada, K., Kimura, K., Abe, F., Taniuchi, Y., Sekido, K., et al. (2019). Catalog of NIMS creep data sheets, *Science & Technology of Advanced Materials*, 20(1), 1131–1149.
- [23] Sawada, K., Kushima, H., Tabuchi, M., & Kimura, K. (2011). Microstructural degradation of Gr.91 steel during creep under low stress, *Material Science & Engineering: A*, 528(16–17), 5511–5518
- [24] Masuyama, F. (2007). Creep rupture life and design factors for high-strength ferritic steels, *International Journal of Pressure Vessels & Piping*, 84(1), 53–61.